AVALANCHE TERRAIN MAPS FOR BACKCOUNTRY SKIING IN SWITZERLAND

Stephan Harvey[1]*, Günter Schmudlach[1,2], Yves Bühler[1], Lukas Dürr[1], Andreas Stoffel[1], Marc Christen[1]

[1] WSL Institute for Snow and Avalanche Research SLF, Davos, Switzerland
[2] Developer and Operator of skitourenguru.ch, Switzerland

ABSTRACT: Terrain characteristics are one of the main factors contributing to avalanche formation. Hence, terrain assessment is crucial for planning and decision making when travelling in the backcountry. So far, terrain is mainly interpreted manually from topographic maps and by observations in the field. Recent support for interpreting avalanche terrain is given by slope angle layers derived from digital elevation models or the Avalanche Terrain Exposure Scale (ATES) for classifying avalanche terrain manually. We developed avalanche terrain maps by combining terrain characteristics of avalanches with the avalanche simulation model RAMMS::EXTENDED and with fall simulations, all based on a high resolution digital elevation model. The focus was on mapping terrain of size class 3 avalanches, which typically threaten backcountry recreationists. We propose a Geographic Information System (GIS) based methodology for a fully automatic classification of the avalanche terrain taking into account: a) potential avalanche release areas, b) remote triggering of avalanches, c) possible runout zones, and d) the potential of being seriously injured or deeply buried by small or medium-sized avalanches. To considered all these aspects several simulations were performed where from we created two different avalanche terrain maps for the entire Swiss Alps and the Jura. One map classifies the avalanche terrain thematically into: i) potential release areas, ii) areas with remote triggering potential, and iii) the runout zones of size 3 avalanches. The second map provides continuous values illustrating how serious or dangerous the terrain is in terms of avalanche release and the consequences of being caught. These maps assist the interpretation of avalanche terrain for travelling in the backcountry. Although they focus on Switzerland, the methods can also be applied to other mountain areas worldwide.

KEYWORDS: avalanche terrain, avalanche terrain map, avalanche hazard mapping, backcountry touring

1. INTRODUCTION

Every year approximately 100 winter sports enthusiasts die in snow avalanches throughout the European Alps (Techel et al., 2016). As most victims trigger the avalanche themselves, evaluating the avalanche danger as well as the exposure is crucial. Terrain plays a major role when assessing the avalanche risk, since it affects both avalanche danger and exposure. Human-triggered avalanches typically release in slightly concave slopes with a 35 degree average slope angle (Vontobel et al., 2013). Terrain also influences the consequences of being caught by an avalanche. Thus, when travelling in the backcountry in winter, avalanche exposure is not only limited to steep slopes. Less steep terrain below has to be considered also regarding remote triggering and the consequences of being caught. Hence, assessing terrain requires more than just evaluating slope angles. Avalanche terrain assessment has to consider potential avalanche release zones and areas at the foot of such slopes with regard to remote triggering, the potential runout zones and the consequences of being caught by an avalanche.

Defining and evaluating avalanche terrain on a map is not straightforward and even experts often interpret terrain differently (Schmudlach et al., 2018). To evaluate, describe, and communicate the complexities of avalanche terrain, Statham et al. (2006) introduced the Avalanche Terrain Exposure Scale (ATES) independent of the current avalanche danger. Using a table with various criteria, a route or a specific location can then be assigned to one of three ATES classes "simple", "challenging" or "complex". The ATES terrain classification system has been adopted in some areas in Europe (e.g. Gavaldà et al., 2013; Pielmeier et al., 2014). However, for the European Alps, the ATES criteria were considered as not ideal, as too many tours would inherently have to be classified as "complex".

So far, backcountry recreationists interpret terrain mainly manually from topographic maps and by observations in the field. Since terrain data are nowadays available numerically in high resolution, it is obvious to support terrain analysis using geographic information systems (GIS). Slope

---

Corresponding author address:
Stephan Harvey, WSL Institute for Snow and Avalanche Research SLF, Flüelastrasse 11,
CH-7260 Davos Dorf, Switzerland,
phone: +41 81 417 01 29, fax: +41 81 417 01 10;
email: harvey@slf.ch

angle maps derived from digital elevation models have become an essential source of information for trip planning in the winter backcountry (Harvey et al., 2016).

A first spatial classification of avalanche terrain using a Geographic Information System (GIS) was conducted by Delparte (2008). Further developments on spatial ATES classification for large areas followed (e.g. Campbell and Gould 2013). None of these GIS-based methodologies are fully automatic, making them less suited for classifying large areas, nor are they highly accurate.

Maggioni and Gruber (2003) and Bühler et al. (2013) determined potential avalanche release areas automatically based on topographic parameters such as slope angle, curvature and ruggedness. Veitinger et al. (2014) presented smoothing factors to better deduce the winter terrain from summer terrain models. However, these automatic approaches only focused on potential release areas. Furthermore, the delineation of the individual release areas, necessary for numerical avalanche simulations, is insufficient (Bühler et al., 2018).

A first approach for a fully automatic spatial terrain evaluation with the focus on backcountry skiing in the Swiss Alps was developed by Schmudlach and Köhler (2016). In contrast to previous work, the algorithm assesses the terrain from the perspective of a skier. A recent study by Thumlert and Haegeli (2017) presented a new methodology for classifying avalanche terrain by exploiting GPS tracks from professional ski guides.

Nevertheless, none of these approaches distinguishes between avalanche release zone, typical areas for remote triggering, avalanche runout zones or the impact of being caught by an avalanche. Assessing these issues is relevant when making decisions in avalanche terrain (Harvey et al., 2018).

Numerical avalanche simulations could make a valuable contribution for evaluating potential runout zones. Indeed, Dreier et al. (2014) showed that the RAMMS avalanche dynamics model (Christen et al., 2010), which was designed for modelling large avalanches (size 4 and 5, McClung and Schaerer 1980), is also suited for simulating smaller skier-triggered avalanches ($\leq$ size 3).

Our goal was therefore to develop avalanche terrain maps (ATM) for typical skier-triggered avalanches (max. size 3) accounting for avalanche release areas, remote triggering, avalanche runout and burial potential and consequences.

The avalanche terrain maps are intended to highlight avalanche specific terrain information rather than just slope angle.

2. DATA AND PROCEDURES

For most terrain analysis we used the digital elevation model swissAlti3D with a resolution of 5 m. From this elevation model we derived different terrain characteristics, such as incline, curvature and a so-called fold feature (Schmudlach and Köhler, 2016), describing the maximum curvature in any direction and therefore characterising relevant terrain changes like ridges and gullies.

2.1 Classifying avalanche terrain

To classify avalanche terrain different steps were necessary. First, terrain characteristics of 5200 mapped avalanche starting zones observed in the region of Davos were analysed. We focussed our analysis on three terrain features, namely incline, curvature and fold. To represent the distribution of the combined occurrence within the avalanche starting zones, a three-dimensional density estimate was computed. With the formulated probability function, we then estimated the probability that any location was within an avalanche starting zone (Harvey et al., 2018, in prep.). Thus, a density layer was created to quantify potential avalanche release areas (Fig. 1).

In a next step, avalanche runout zones were calculated with the avalanche simulation model RAMMS::EXTENDED (Bartelt et al., 2012, 2016). This model simulates the runout of an avalanche taking into account the terrain for a defined release area (polygon) including the extent and predefined input variables, e.g. fracture depth. To make this possible over the entire area of the Swiss Alps, polygons of potential avalanche release areas were calculated automatically with a recently suggested object-based approach (Bühler et al., 2018). Then, RAMMS simulations were carried out for each of these release areas. Overall, approximately 860,000 individual avalanche simulations were thus performed. To limit the number of simulations, we excluded very small slopes from the RAMMS simulations. For these slopes, we then applied a simple slope gradient approach to estimate the runout of these potential tiny avalanches.

The potential of remote triggering was estimated by analysing a data set of 75 human triggered avalanches with known distances from the triggering point to the release area to compute the remote triggering probability with distance. This distribution was combined with the profile curvature, assumed to influence crack propagation, to create a cost matrix as input for the ArcGIS tool "path distance" (ESRI, 2018). The path distance calculation started with the weighted density values from the release areas. The resulting values were classified into three groups and assigned a bluish colour (Fig. 2). Only values within the

simulated avalanche runout zones were taken into account.

2.2 *Estimating consequences*

Being caught by an avalanche can either lead to burial and therefore to danger of suffocation and/or result in serious injuries. To model these possible consequences, we focused on burial depth and falling potential.

Potential for deep burial: Each RAMMS simulation approximated an avalanche deposit depth. We assumed that for deeper deposits the slopes above were more dangerous. To account for this, we again used the "path distance" function to calculate the potential for burial at a certain location uphill from the deposit. For this calculation, the distance to the deepest burial depth and the largest avalanche pressure of the simulated avalanches were used to construct a cost matrix. Locations in the upper part of a slope with lower pressure from the avalanche therefore had less burial potential. For each cell, a normalized burial potential over all simulations was thus assigned.

Potential for serious injury from a large fall: To estimate the consequences of a fall, trajectories with a maximum length of 1000 m were calculated in the fall line direction, using a 10 m elevation model. Velocities and accelerations were determined along these trajectories. At concave cells, slope perpendicular accelerations and high velocities can lead to injury. For both, the sum and the maximum values of the calculated accelerations and velocities along each trajectory, a threshold value was determined above which fatal injuries were assumed. The values between 0 and these thresholds were normalized for each of the two parameters. The higher value of these two parameters was then assigned to each raster cell as an indicator of injury potential from a fall.

Finally, the burial and fall potential were combined to create a raster-based layer describing the consequences of being caught by an avalanche (Fig. 1).

3. AVALANCHE TERRAIN MAPS

From the spatial calculations described above, several raster layers were derived for the whole of Switzerland (Fig. 1). These were combined in two different ways to create intuitive avalanche terrain maps.

3.1 *Classified potential avalanche terrain*

The first map divides avalanche terrain thematically into potential release areas (red colours) and runout zones (blue and yellow; Fig. 2). For the release areas, only terrain with a slope angle between 30 and 50 degrees was considered. The calculated density values within these areas were

then divided into 4 classes, with darker red colours indicating terrain more frequently associated with avalanches. The two highest classes represent 2/3 of all release areas in our data set of 5200 mapped avalanches.

Potential runout zones are coloured in three shades of blue and yellow. The darker the blue, the higher the remote-triggering potential. The yellow colours show the maximum runout of a size 3 dry-snow slab avalanche with an average fracture depth of 50 cm. Assuming that an avalanche is remotely triggered, the relative probability is between 50 and 100% for dark blue, between 20 and 50% for medium blue and between 1 and 20% for light blue. In the yellow colour, the remote triggering is very unlikely (probability <1%).

This map does not consider the consequences of being caught by an avalanche.
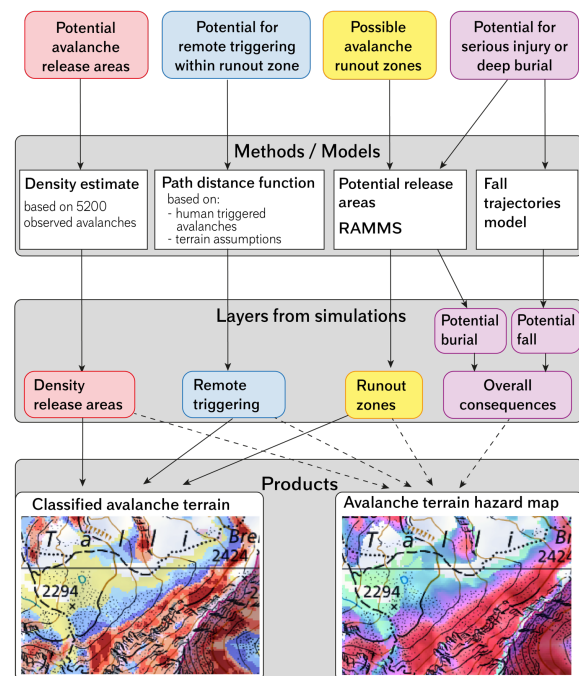

Fig. 1: Workflow for creating the two avalanche terrain maps.

3.2 *Potential avalanche terrain hazard*

To create the second map (Fig. 3), we combined avalanche terrain with potential consequences. The continuous values characterizing the avalanche terrain resulted from the calculations for the remote triggering potential. Since the initial starting values for the "path distance" calculation were derived from the density values of the release areas, the release areas are included in the remote triggering output layer. These values were normalized and combined with the normalized consequences layer to create a new avalanche terrain hazard layer (Fig. 3). This layer

describes the severity of the terrain with regard to the release and the consequences of an avalanche and was calculated by:

$$H = \sqrt{r \times c} \qquad (1)$$

where H = avalanche terrain hazard; r = terrain potential for triggering an avalanche; c = consequences of being caught by an avalanche.

In contrast to the first map, it is no longer possible to clearly distinguish between potential release areas and areas with remote triggering potential. The calculated values for potential avalanche release, remote triggering potential, runout as well as the possible consequences of burial or fall were merged together and described by continuous value between 0 and 1. The higher the value the more dangerous the terrain. For instance, a location in a typical release area above a gently slope may have a similar value as a location where the terrain is convex and less typical for avalanche release but above a terrain feature with fatal consequences when falling (e.g. above a cliff).

3.3 Limitations

Obviously these automatically generated maps have some limitations and the following points have to be considered:

−   The focus was on typical human-triggered avalanches up to and including avalanche size class 3.

−   Forest classified as "dense" was not considered, whereas forest classified as "open" was treated as un-forested terrain. In reality forest structure is dynamic leading to potential errors.

−   Aspect and elevation were not considered, except that there were no RAMMS simulations below 1000 m.

−   Slope angles above 50 degrees were not considered.

−   Areas that are not coloured are relatively safe as far as the hazard of up to size 3 avalanches is concerned. While narrow ridges are often not coloured (i.e. rather safe), such areas may be dangerous due to other hazards such as cornices, risk of falling etc.

Release areas

■ high potential
■ medium potential   ⎤ 2/3 of all
■ low potential   ⎦ release areas
■ very low potential

Runout zones for size 3 avalanches

■ high potential for remote triggering
■ medium potential for remote triggering
■ low potential for remote triggering
■ max. runout; remote triggering is very seldom or unlikely

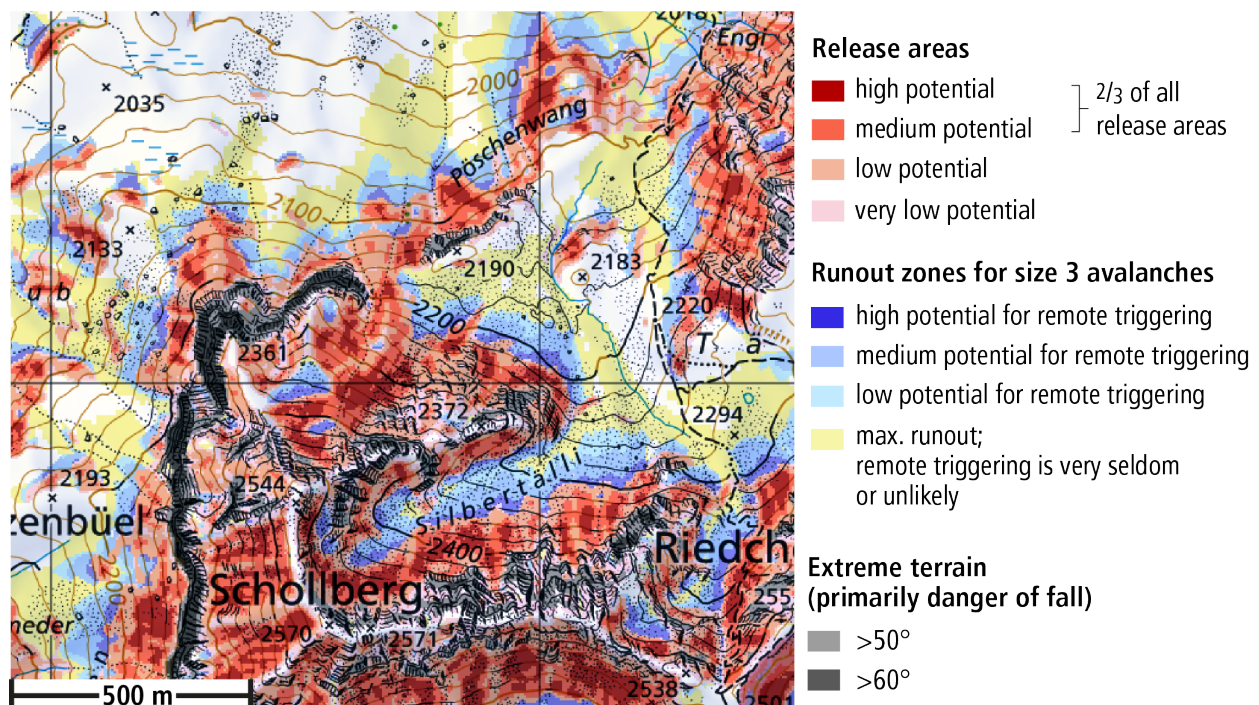**Extreme terrain (primarily danger of fall)**

■ >50°
■ >60°

Fig. 2: Classified avalanche terrain distinguishing between avalanche release area and runout zones for max. size 3 avalanches.
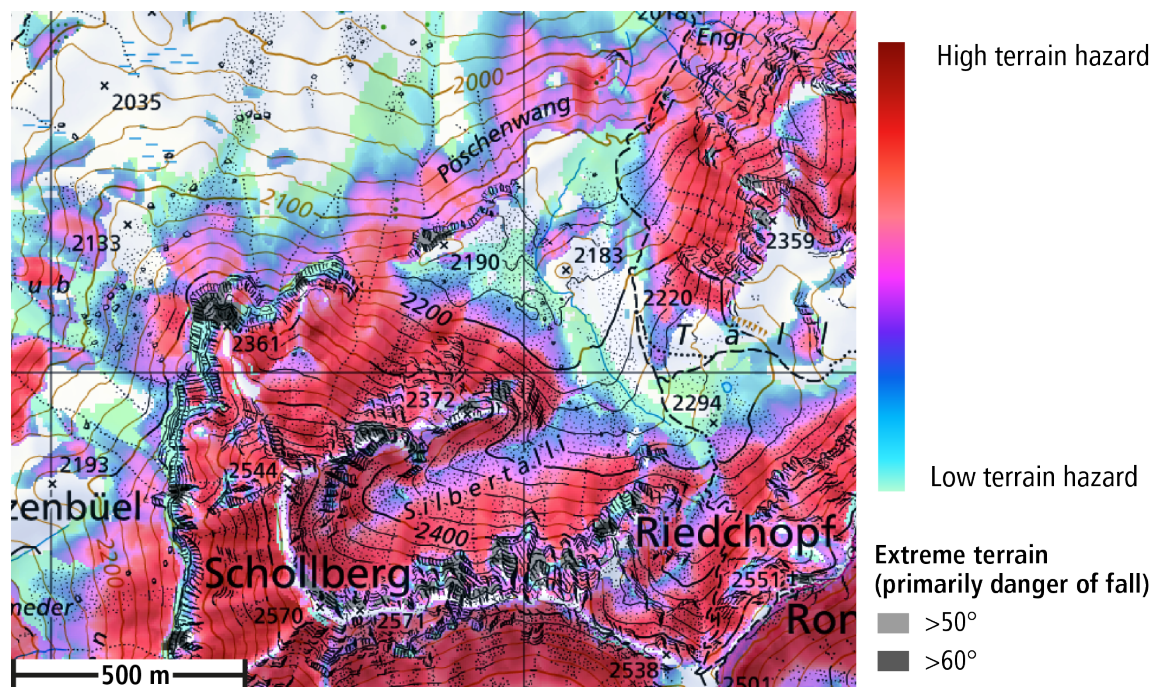
Fig. 3: Avalanche terrain hazard map describing the terrain hazard with continuous values for max. size 3 avalanches.

4. DISCUSSION

We automatically classified avalanche terrain with high spatial resolution for the entire Swiss Alps and the Jura based on quantitative data and models. Using a large data set of mapped avalanches, we derived density estimates based on topographic parameters for potential avalanche release areas. Uniform or slightly concave slopes with slope angles around 35 degrees were most avalanche prone, whereas convex and irregular steeper slopes were less frequently associated with avalanche release areas. These results correspond to findings of Vontobel et al. (2013) and confirm that slope angle is not the only terrain variable characterizing potential release areas. To model the potential areas for remote triggering, we relied on a small dataset of remotely triggered avalanches that suggests a rapid decrease of remote triggering potential with distance to the release area. However, the highlighted potential for remote triggering requires "ideal" conditions for triggering avalanches remotely and thus corresponds to a very unfavourable scenario.

RAMMS simulations were performed to estimate the runout distance and potential burial depth of typical human-triggered avalanches. Although these simulations were only performed for one avalanche situation, the results are promising. Comparing the perimeters of 5200 observed avalanches showed that only 4.7% of the total avalanche perimeters flow further than the simulated runout zones. This indicates that the modelled runout zones are rather conservative for typical human-triggered avalanches. Due to restricting the size of the potential release areas for the RAMMS simulations, large slopes were split into several smaller release areas. On such large slopes, the modelled runout is therefore likely underestimated. Furthermore, in some cases the runout distance of avalanches from small slopes was somewhat overestimated.

Evaluating terrain in terms of an avalanche release is only one part of risk assessment. Accounting for the consequences of being caught by an avalanche is equally important. In real terrain, these consequences are relatively obvious to assess, in contrast to the avalanche release potential. We thus applied an approach to identify terrain traps automatically. The two different procedures used to consider burial and fall potential are rather simplistic and improvements could be made by specific modelling of the impact of avalanches with RAMMS.

By focussing on i) release areas, ii) remote triggering, iii) runout, and iv) consequences, we created different raster-based layers. These were combined in two different ways to classify avalanche terrain and to automatically create intuitive maps for the entire Swiss Alps and the Jura.

The first map (classified avalanche terrain, Fig. 2) is of semantic nature and differentiates potential release area, potential remote triggering areas and runout zones. Hence, the classification in this map contains qualitative and quantitative information. However, the consequences of being caught by avalanches were not incorporated. Within the classes of avalanche release areas

(red colours) and runout zones (blue and yellow colours) respectively, a rating is possible. Comparing both classes is however not possible. Depending on the current avalanche situation, the two main classes have to be interpreted and assessed separately.

The second map (Avalanche terrain hazard map, Fig. 3) contains continuous values from 0 to 1 indicating the overall avalanche hazard arising from the terrain. These values also include the consequences of being caught by an avalanche. While in such a map it is not possible to determine why a specific value was obtained, this map is easier to interpret by inexperienced recreationists as serious terrain in terms of avalanche hazard can quickly be identified. Furthermore, this map is suitable for further machine processing.

5. CONCLUSIONS

The presented, high resolution avalanche terrain classification is suitable for Alpine regions. It should be noted that the calculations are optimised for situations within the range of avalanche danger levels "2: Moderate" to "3: Considerable". The focus is on human-triggered avalanches up to and including size 3. Snow cover conditions are not included in both these maps. Unlike Eisenhut (2013) the maps also do not give information about the accessibility and difficulty of travelling in the terrain.

Both maps can be applied in the same manner as the widely used slope angle layers. While aspect and elevation are not considered, the presented maps provide insight into typical avalanche terrain and focus on important issues such as avalanche release, triggering, runout as well as potential consequences. We plan to make the maps available to the general public next winter.

These maps or other combinations of the resulted layers provide a solid foundation to describe avalanche terrain for any future developments, e.g. classifying routes, real time hazard mapping etc.

6. ACKNOWLEDGEMENTS

REFERENCES

Bartelt, P., Bühler, Y., Buser, O., Christen, M., Meier, L., 2012. Modeling mass-dependent flow regime transitions to predict the stopping and depositional behavior of snow avalanches, Journal of Geophysical Research, 117(F1), doi:10.1029/2010JF001957.

Bartelt, P., Buser, O., Valero, C.V., Bühler, Y., 2016. Configurational energy and the formation of mixed flowing/powder snow and ice avalanches, Annals of Glaciology, 57(71), 179 - 188, doi:10.3189/2016AoG71A464.

Bühler, Y., von Rickenbach, D., Stoffel, A., Margreth, S., Stoffel, L., Christen, M., 2018. Automated snow avalanche release area delineation - validation of existing algorithms and proposition of a new object-based approach for large scale hazard indication mapping, Natural Hazards and Earth System Science Discussion, doi:10.5194/nhess-2018-124.

Bühler, Y., Kumar, S., Veitinger, J., Christen, M., Stoffel, A., and Snehmani, 2013. Automated identification of potential snow avalanche release areas based on digital elevation models, Nat. Hazards Earth Syst. Sci., 13, 1321-1335.

Campbell, C. and Gould, B., 2013. A proposed practical model for zoning with the Avalanche Terrain Exposure Scale. In: F. Naaim-Bouvet, Y. Durand and R. Lambert (Editors), Proceedings ISSW 2013. International Snow Science Workshop, Grenoble, France, 7-11 October 2013. ANENA, IRSTEA, Météo-France, Grenoble, France, pp. 385-391.

Christen, M., Kowalski, J., and Bartelt, P., 2010. RAMMS: Numerical simulation of dense snow ava-lanches in three-dimensional terrain, Cold Reg. Sci. Technol., 63, 1-14.

Delparte, D., 2008. Avalanche terrain modeling in Glacier National Park, Canada. Ph.D. thesis, Department of Geography, University of Calgary, Canada.

Dreier, L., Bühler, Y., Steinkogler, W., Feistl, T. and Bartelt, P., 2014. Modelling small and frequent avalanches. In: P. Haegeli (Editor), Proceedings ISSW 2014. International Snow Science Work-shop, Banff, Alberta, Canada, 29 September - 3 October 2014, pp. 649-656.

Environmental Systems Research Institute (ESRI) ArcGIS software. 2018. http://desktop.arcgis.com/en/arcmap/latest/tools/spatial-analyst-toolbox/path-distance.htm

Eisenhut, A., 2013. Skitourenplanung auf Knopfdruck? Die optimale Aufstiegsroute bezüglich Anstrengung und Lawinensicherheit, modelliert mit einem Geographischen Informationssystem (GIS). Zur Erlangung des Grades Master of Science (Geographical Information Science and Systems) – MSc (GIS)

Gavaldà, J., Moner, I., Bacardit, M., 2013. Integrating ATES into the avalanche information in Aran Valley (Central Pyrenees). In: Proceedings of the 2013 international snow science workshop, Grenoble, France, pp 381–384

Harvey, S., Rhyner, H., Dürr, L., Schweizer , J., Henny, H., Nigg, P., 2016. Leaflet "Caution Avalanches". Swiss Core Training Team for Avalanche Prevention KAT. https://www.slf.ch/en/publicationssearch/books-and-brochures.html

Harvey, S., Rhyner, H., Dürr, L., Henny, H.M., 2018. To go or not to go: Decision making at individual slope. In: Proceedings of the 2018 international snow science workshop, Innsbruck, Austria.

Harvey, S., Schmudlach, G., Bühler, Y., Dürr, L., Stoffel, A., Christen, M. in prep. Automatic high-resolution mapping and classification of avalanche terrain.

Maggioni, M. and Gruber, U., 2003. The influence of topographic parameters on avalanche release dimension and frequency, Cold Reg. Sci. Technol., 37, 407-419.

McClung, D. and Schaerer, P., 1980. Snow Avalanche Size Classification. Proceedings ISSW 1980. International Snow Science Workshop, Vancouver BC, Canada, 29 November 3-5, pp. 12-30.

Pielmeier, C., Silbernagel, D., Dürr, L. and Stucki, T., 2014. Applying the avalanche terrain exposure scale in the Swiss Jura mountains. In: P. Haegeli (Editor), Proceedings ISSW 2014. International Snow Science Workshop, Banff, Alberta, Canada, 29 September - 3 October 2014, pp. 883-889.

Schmudlach, G., Köhler J., 2016. Method for an automatized avalanche terrain classification. In: Proceedings of the 2016 international snow science workshop, Breckenridge, USA, pp 729–736

Schmudlach, G., Harvey, S., Dürr, L., 2018. How do experts interpret avalanche terrain from a map? In: Proceedings of the 2018 international snow science workshop, Innsbruck, Austria.

Statham, G., McMahon, B., Tomm, I., 2006. The avalanche terrain exposure scale. In: Proceedings of the 2006 international snow science workshop, Telluride, USA, pp 491–499

Techel, F., Jarry, F., Kronthaler, G., Mitterer, S., Nairz, P., Pavšek, M., Valt, M., Darms, G. 2016. Avalanche fatalities in the European Alps: long-term trends and statistics. Geogr. Helv., 71, 147–159, 2016 www.geogr-helv.net/71/147/2016/ doi:10.5194/gh-71-147-2016

Veitinger, J.; Sovilla, B.; Purves, R.S., 2014. Influence of snow depth distribution on surface roughness in alpine terrain: a multi-scale approach. Cryosphere, 8, 547-569.

Vontobel, I., Harvey, S. and Purves, R.S., 2013. Terrain analysis of skier-triggered avalanche starting zones. In: F. Naaim-Bouvet, Y. Durand and R. Lambert (Editors), Proceedings ISSW 2013. Inter-national Snow Science Workshop, Grenoble, France, 7-11 October 2013. ANENA, IRSTEA, Météo-France, Grenoble, France, pp. 371-375.